Radio pulsar activity and the crustal Hall drift

U. Geppert[1,2]*, J. Gil[1], G. Melikidze[1,3]
[1] *Kepler Institute of Astronomy, University of Zielona Góra, Lubuska 2, 65-265, Zielona Góra, Poland*
[2] *German Aerospace Center, Institute for Space Systems, , Robert-Hooke-Str. 7, 28359 Bremen, Germany*
[3] *Abastumani Astrophysical Observatory, Ilia State University, 3-5 Cholokashvili str., Tbilisi, 0160, Georgia*

ABSTRACT
Models of pulsar radio emission that are based on an inner accelerating region require the existence of very strong and small scale surface magnetic field structures at or near the canonical polar cap. The aim of this paper is to identify a mechanism that creates such field structures and maintains them over a pulsar's lifetime. The likely physical process that can create the required 'magnetic spots' is the Hall drift occurring in the crust of a neutron star. It is demonstrated, that the Hall drift can produce small scale strong surface magnetic field anomalies (spots) on timescales of 10^4 years by means of non-linear interaction between poloidal and toroidal components of the subsurface magnetic field. These anomalies are characterized by strengths of about 10^{14} G and curvature radii of field lines of about 10^6 cm, both of which are fundamental for generation of observable radio emission.

Key words: stars: pulsars: general – stars: magnetic field

1 INTRODUCTION

About 45 years after the discovery of the first radio pulsars the physics of the generation of the radio emission is still a subject of intense scientific debates. There is a general agreement that the strong potential drop above the polar cap surface must exist to accelerate the charged particles to ultra-relativistic energies. Two pioneering papers by Ruderman & Sutherland (1975) and by Arons & Scharlemann (1979) started an intensive research in two different classes of models: non-stationary (sparking gap) and stationary (free flow), respectively. Observational and theoretical evidences are searched for and studied to support or discard one or the other model. The phenomenon of drifting sub-pulses and the combined observations of pulsars in radio and X-rays (Gil et al. 2007a,b, 2008) support strongly the idea that the Partially Screened Gap (PSG hereafter, Gil et al. 2003) is the case, in which the pure vacuum potential drop is partially screened by thermal iron ions (Cheng & Ruderman 1977).

The creation of a dense electron-positron plasma is the basis of pulsar radio emission processes. These pairs can be created by photons originating from inverse Compton scattering and/or from curvature radiation, both interacting with a very strong and curved magnetic field as compared to the global dipolar field B_d at the surface. Therefore, the small scale field has to be generated in the crust of the neutron star. Already Ruderman & Sutherland (1975) in their pioneering work on the inner acceleration gap noticed implicitly a necessity of small scale surface magnetic field with the radius of curvature of about 10^6 cm, much smaller than 10^8 cm that is

typical for the global dipole field. These authors, however, did not specify a mechanism that could generate such a field structure at the polar cap. In our paper we explore whether the Hall drift can play that role.

To build up an accelerating potential drop in the polar gap the cohesive energy of charges at the polar cap surface has to exceed some critical value. This will prevent particles from escaping the stellar surface. As soon as the electric field exceeds a certain threshold an avalanche pair creation discharges the ultrahigh gap potential drop. The cohesive energy ϵ_c is strongly dependent on the surface magnetic field strength B_s, which should be much stronger than B_d. As demonstrated by Medin & Lai (2007), who performed calculations for helium, calcium and iron atoms at the surface, for each value of the magnetic field B_s there is a a critical temperature T_s above which the accelerating gap cannot be formed. This critical temperature and corresponding cohesive energy are represented by the red line in Fig. 1 connecting the data points taken from the paper of Medin & Lai (2007). No gap can exist above this line and pure vacuum gap is possible below it. The PSG with some amount of thermally released iron ions can exist in a narrow region along the red line (see section 2 for more details).

X-ray observations of radio pulsars (see e.g. Zhang et al. 2005; Kargaltsev et al. 2006; Gil et al. 2008; Pavlov et al. 2009) indicate that a polar cap surface is strongly heated due to the bombardment with back flowing charges accelerated within a polar gap. Given the magnetic field dependence on the cohesive energy, the actual field strength necessary to form a gap has to be much stronger than global dipolar field B_d. These observations estimate the size of the bombarded area ('hot spot') being less then 100 m, suggesting a locally very small scale field. This strong and small scale field

* E-mail:ulrich.geppert@dlr.de

anomaly, the 'magnetic spot', is obviously located within or close to the conventional polar cap area introduced by Goldreich & Julian (1969). The actual polar cap ('hot spot') is the locus of those anomalous magnetic field lines that join with the open dipolar field lines at some higher altitudes (Gil, Melikidze & Mitra 2002). The surface area of this actual polar cap is at least one order of magnitude smaller then the conventional polar cap. The black-body temperature of the 'hot spot' is estimated to exceed one Million Kelvin, which indicates very strong surface magnetic fields close to or even above 10^{14} G (see Fig. 1).

While the PSG model explains quite well the variety of pulsar observations both in radio and X-ray bands, a missing link is a process that can create and maintain the required strong and small scale surface magnetic field structures over the lifetime of radio pulsars, i.e. $\sim 10^6 - 10^7$ years. These structures should have high strength $B_s > 5 \times 10^{13}$ G to provide high enough cohesive energy to form PSG, and have small radius of curvature $R_{\rm cur} \sim 10^6$ cm to cause creation of large enough number of electron-positron pairs to generate the coherent observable radio emission by means of some kind of plasma instabilities (Pataraia & Melikidze 1980; Asseo & Melikidze 1998; Melikidze et al. 2000; Gil et al. 2004).

In this paper we will describe in some detail the idea that the Hall drift of the crustal magnetic field could generate the required surface field structures out of a strong ($\sim 10^{15}$G) toroidal field component, which has been formed immediately after birth of the neutron star. For simplicity we assume that it has an axisymmetric geometry. The currents maintaining this field circulate in deep crustal layers, where the high electric conductivity guarantees lifetimes well exceeding 10^6yrs. This mechanism has been proposed recently by Geppert et al. (2012) and will be discussed here in extenso. The purpose of this paper is not to present a set of models that describe exactly the creation of the required 'magnetic spots'. On the currently available level of modeling the magneto-thermal evolution (2D computations only) such description is not yet possible. Rather, we want to introduce a mechanism that is apparently able to maintain the required magnetic structures over a pulsar lifetime.

In Section 2 basic ideas of the PSG model will be explicated. Observational indications for the size of the magnetic spot in the polar cap, the corresponding surface field strength there and its surface temperature will be discussed. Processes and conditions for the creation of electron-positron pairs as well as the estimates for the necessary magnetic field scales will be described in Section 3. In Section 4. we will discuss possible processes that might create 'magnetic spots' and argue in favor of the Hall drift. The role of the 'initial' magnetic field configuration will be examined. The magneto-thermal evolution in the crystallized crust and the obtained results for the creation of 'magnetic spots' are presented in Section 5. These spots are characterized by their surface field strengths and the curvature radius of their field lines. These characteristic quantities are results of the numerical solution of the Hall induction equation, assuming state of the art crustal micro-physics, equation of state, and an initial crustal field configuration that consists of a strong ($\sim 10^{15}$G) toroidal component and a dipolar field standard for radio pulsars ($\sim 10^{12} - 10^{13}$G). In Section 6 we summarize the results as well as discuss the necessary extension of the model to non-axial symmetric configurations.

2   THE PARTIALLY SCREENED GAP MODEL

The PSG model (Gil et al. 2003) is an refinement of the vacuum gap model developed by Ruderman & Sutherland (1975). If the electron-positron pair production really occurs in the inner accelerator potential drop, then one should expect an intense thermal radiation from the hot polar cap. Indeed, the accelerated positrons will leave the acceleration region, while the electrons will bombard the polar cap surface, causing heating of the polar cap surface to MK temperatures. At the same time thermal ejection of iron ions should occur, which will partially screen the polar cap electric field. This is the essence of the PSG pulsar model. The pure vacuum gap produces too much thermal X-ray emission, in contrast with observations, so the PSG model is a natural and expected advancement.

In order for the PSG model to function it requires high enough cohesive energy of iron ions to bind them at least partially at the polar cap surface. We refer to the most recent calculations of cohesive energies by Medin & Lai (2007) represented by the curved line in Fig.1. As shown by these authors the critical surface temperature T_i , below which the PSG can form, depends strongly on the actual surface magnetic field B_s, that must be close to 10^{14} G in all pulsars for which the surface temperature (T_s) of their heated polar cap exceeds 10^6 K. This is strongly suggested by X-ray spectral observations of a number of pulsars shown in Fig. 1. Both the critical T_i and the actual T_s temperatures must be close to each other by means of the thermostatic regulation mechanism. Indeed, if T_i is slightly higher than T_s, then heating by the bombardment becomes more intense, consequently increasing the surface temperature thus making heating less intense. This is a classical thermostat mechanism, which will set $T_s \sim T_i$ in PSG along the red line and its nearest vicinity (see discussion in Section 6) presented in Fig. 1.

The parameters of the black body fit to the X-ray spectrum of some pulsars provide very important information for the understanding of the physical conditions at the neutron star surface. The black body fit allows us to obtain directly both the 'hot spot' area $A_{\rm BB}$ and its temperature $T_{\rm BB}$. In most cases $A_{\rm BB}$ is much smaller than the conventional polar cap area $A = 6.6 \times 10^8 P^{-1}$ cm^2, where P is the pulsar period (see Zhang et al. 2005; Kargaltsev et al. 2006). This can be easily explained by assuming that the surface magnetic field of pulsars B_s differs significantly from the surface value of the global dipole $B_d(R)$, where R is the neutron star radius. Then, one can estimate an actual surface magnetic field by the magnetic flux conservation law as $b = A/A_{\rm BB} = B_s/B_d$, where $B_d = 2 \times 10^{12}(P\dot{P}_{-15})^{0.5}$ G is the dipolar magnetic field at the polar cap surface, $\dot{P}_{-15} = \dot{P} \times 10^{-15}$ and $\dot{P}$ is the period derivative. Then the value of the actual surface magnetic field at the hot polar cap can be expressed as

$$B_s = 1.3 \times 10^{21} A_{\rm BB}^{-1} (P\dot{P}_{-15})^{0.5} G, \tag{1}$$

where $A_{\rm BB}$ is 'hot spot' area. In most cases $b >> 1$ implying $B_s >> B_d$, while $T_{\rm BB} \sim (2-4) \times 10^6$ K. This is shown in Fig. 1 , which also confirms observationally the cohesive energy calculations performed by Medin & Lai (2007). Indeed, the data points and their errors represent a number of pulsars in which estimation of the surface area (thus the surface magnetic field) and the surface temperature were possible from X-ray observations (e.g. Szary 2013). They all lie close to and on the right side of the PSG line in the region where gap formation is possible. The estimated surface magnetic field B_s exceeds slightly 10^{14} G for all data points. The exemplary values of the dipolar surface magnetic field correspond-
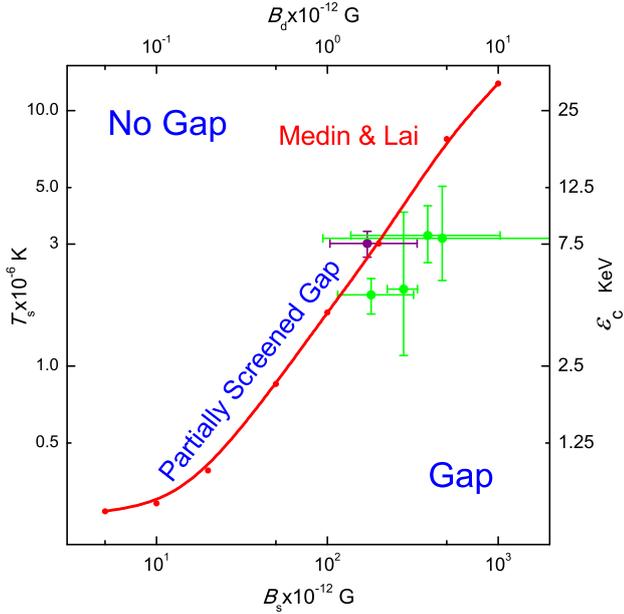
Figure 1. Conditions for the creation of a vacuum gap above polar cap surface layers consisting of iron (according to Medin & Lai (2007)) with given surface temperature T_s and surface magnetic field B_s. For an iron surface temperature $T_s > 10^6$K, surface field strength of $B_s \gtrsim 10^{14}$G is necessary (for carbon and helium surfaces the conditions are even more stringent). PSG can be formed in a narrow belt along the red line. Green data points and their error bars come from various sources (see e.g. Szary 2013, and references therein), while the purple dot and corresponding error bars for PSR B0943+10 are extracted from Table 3 in the newest paper by Mereghetti et al. (2013, see also discussion in the text below).

ing to $b = A/A_{BB} = B_s/B_d$ taken as 100 are shown on the upper abscissa.

For typical radio pulsar parameters with $T_s \gtrsim 2 - 3 \times 10^6$K which implies, that a vacuum gap can only be formed if B_s exceeds 10^{14}G. Flux conservation arguments relate the area of the polar cap encircled by the last open field lines to the black-body area estimated from X-ray observations. Zhang et al. (2005) and Kargaltsev et al. (2006) found $B_s \approx 4 \times 10^{14}$ G, $T_s \approx 3 \times 10^6$ K for PSR B1133+16 while its dipolar field derived from P and $\dot{P}$ is $B_d \approx 4 \times 10^{12}$G. Analogously $B_s \approx 2 \times 10^{14}$ G, $T_s \approx 3 \times 10^6$ K for PSR B0943+10, while for its dipolar component $B_d \approx 6 \times 10^{12}$ G at the polar cap. These estimates, based on combined radio and X-ray observations of isolated neutron stars, indicate the existence of a small scale but very strong magnetic field B_s that is concentrated in an indeed 'hot spot' within or very close by to the conventional pulsar polar cap (see Fig. 1 in Szary et al. 2010). Although the photon statistics is rather poor in these observations, the conclusions about the small sizes and high T_s of these spots are strongly supported by the theoretical arguments of the balance of cooling and heating by bombardment with ultra-relativistic particles. Moreover, the recent long time exposure observations of B0943+10 by XMM-Newton (Hermsen et al. 2013) leave no doubt about the existence of very small hot spots associated with the polar cap of radio pulsars.

Now we can give a good example of PSG model application to a real pulsar. We have just came across the new paper by Mereghetti et al. (2013), in which the authors reanalyze good quality data taken during simultaneous observations of PSR B0943+10 in radio and X-ray bands (Hermsen et al. 2013). This old (5 Myr) pulsar with $P = 1.1$ s and $\dot{P}_{-15} = 3.5$ is known for a very regular subpulse

drift in the so called B-mode. Mereghetti et al. (2013) found that the X-ray emission in the B-mode of PSR B0943+10 is well described by thermal emission with blackbody temperature $T_s = 3 \times 10^6$ K coming from a small hot spot (with R_{BB} of about 20 m, much smaller than the canonical polar cap radius $R_{PC} = 140$ m) with luminosity of 7×10^{28} erg/s, in good agreement with predictions of PSG (Gil et al. 2003, 2008). Indeed, for $A_{BB} = 1.4 \times 10^7$ cm^2 Eq. (1) gives the value of the surface magnetic field $B_s = 1.7 \times 10^{14}$ G, much bigger than the dipolar surface component $B_d = 4 \times 10^{12}$ G. The case of PSR B0943+10 is marked in Fig. 1 as the purple dot with co-ordinates $x = 1.71 \times 10^{12}$ and $y = 3.02$, which lies exactly at the theoretical line of Medin & Lai (2007). Thus, the small size of the detected hot spot (the size of the actual polar cap) is naturally and self-consistently explained by the magnetic flux conservation law expressed by Eq. (1). The ultra-strong surface magnetic field required by the cohesive energy needed to form PSG in PSR B0943+10 can be indeed inferred from the detected X-ray data. In this paper we argue that such strong magnetic field anomalies can be naturally generated by the Hall drift effect.

3 THE ELECTRON-POSITRON PAIR CREATION

The creation of a large enough number of electron-positron pairs is a basic prerequisite for models that claim to explain the generation of the pulsar radio emission (e.g. Ruderman & Sutherland 1975; Arons & Scharlemann 1979; Gil et al. 2004). Depending on the kind of radiation that produces pairs with the bystander of the magnetic field, certain conditions have to be fulfilled. In the following we describe in some detail processes of electron-positron pair creation and derive the requirements to be placed on strength and curvature of the surface magnetic field B_s.

Basically, there are two kinds of high-energy γ seed photons that can take part in the pair creation in the presence of a strong magnetic field: the curvature radiation (CR) and the inverse Compton scattering (ICS) photons. Let us discuss the CR photons first. There are two main parameters that affect the efficiency of CR pair creation process: the particle (electron and/or positron) mean free path l_p (before it emits a γ photon) and the photon mean free path (before this photon converts into a pair). The smaller these paths are the more efficient the pair creation process is. According to Zhang et al. (1997)

$$l_p = l_{CR} \sim \frac{2\hbar c}{\gamma e^2} R_{cur} \,, \tag{2}$$

where R_{cur} is the curvature radius of magnetic field lines. Thus, while passing a distance l, the particle can emit approximately l/l_{CR} photons with energy $E_\gamma = h\nu_{CR} \approx 1.4 \times 10^{-17}\gamma^3/R_{cur}$ (see Jackson 1975). Part of the particle energy that is transferred into radiation ϵ is given by

$$\epsilon = \frac{E_\gamma}{\gamma m_e c^2} \frac{l}{l_{CR}} \approx 2 \times 10^{-13} \frac{\gamma^3}{R_{cur}^2} l \,. \tag{3}$$

On the other hand, the photon with the energy $E_\gamma > 2mc^2$ propagating obliquely to magnetic field lines can be absorbed by the field and as a result an electron-positron pair is created. Thus, the photon free path l_{ph} can be estimated as a mean distance which a photon should cover until it is absorbed by a magnetic field. For strong magnetic fields ($B \gtrsim 0.2B_q$, see Ruderman & Sutherland 1975, for definition of B_q) the photon mean free path can be calculated

as

$$l_{\mathrm{ph}} \sim \frac{2mc^2}{E_\gamma} R_{\mathrm{cur}} = 1.2 \times 10^{11} \frac{R_{\mathrm{cur}}^2}{\gamma^3}. \qquad (4)$$

For typical pulsar magnetic fields the dipolar radius of curvature is of the order of 10^8 cm. Thus, for Lorentz factors $\gamma < 5\times10^6$ we get from Eqs. 3 and 4 that $\epsilon < 2.5 \times 10^{-9}l$. Therefore, even passing a distance of $l \sim R = 10^6$ cm, where R is the NS radius, a particle will transfer much less than 1% of its energy into curvature radiation. The photon free path l_{ph} for the same parameters is about $l_{\mathrm{ph}} \sim 10^7$ cm, much too long to assure the effective pair creation inside the gap with height smaller than 100 m.

To get a reasonable level of pair production, the radius of curvature has to be decreased by two or three orders of magnitude, i.e. $R_{\mathrm{cur}} \sim 10^{5-6}$cm, e.g. assuming $R_{\mathrm{cur}} = 5 \times 10^5$cm, we find $\epsilon \approx 10^{-4}l$ cm and $l_{\mathrm{ph}} \sim 2 \times 10^2$ (Eqs. 3 and 4), i.e. the particle transfers a substantial part of its energy while passing less than 100 m (a gap height) and the emitted curvature photons are converted into electron-positron pairs. Therefore, Eqs. 3 and 4 demonstrate that the efficiency of the pair creation (i.e. ϵ and l_{ph}) is very sensitive to the curvature of magnetic field lines and thus a small scale B_s with a typical $R_{\mathrm{cur}} \lesssim 10^6$cm is necessary for the efficient pair creation, as already suggested by Ruderman & Sutherland (1975).

The resultant magnetic field at the polar cap is a vector sum of two components: star centered global dipole field and crust anchored small scale field. In order to get the radius of curvature close to the surface sufficiently small ($< 10^6$cm), the small scale field has to be much stronger than the dipolar component close to the surface.

For the Inverse Compton Scattering (ICS) process calculation of the particle mean free path l_{ICS} is not as simple as for that of the curvature radiation. Although we can define l_{ICS} in a same way as we have defined l_{CR}, it is difficult to estimate a characteristic frequency of emitted photons. We have to take into account photons of various frequencies with various incident angles.

One should expect two modes of ICS, resonant and thermal-peak. Under the gap conditions the cross-section of the resonant ICS is much bigger then the cross-section of the thermal ICS. The resonant ICS happens if the photon frequency in the particle rest frame equals to the electron cyclotron frequency, i.e. a magnetic field B_s should be strong enough to satisfy the resonant condition for X-ray photons. Detailed calculations demonstrate that again B_s has to be of the order of $10^{13} - 10^{14}$ G within a gap (see Szary 2013).

4   PROCESSES THAT CAN CREATE STRONG SMALL SCALE MAGNETIC FIELD STRUCTURES AT THE POLAR CAP

As shown in the preceding sections, the 'magnetic spot' has to consist of strong and small scale, i.e. very curved, components of the surface magnetic field. These structures have to be present for at least $\sim 10^6$yrs. These two requirements have to be fulfilled in spite of the facts, that the ohmic lifetime of such small field structures is significantly smaller than that of the global dipolar field which is maintained by currents circulating in the highly conducting deep regions of the crust and/or in the perhaps superconducting core.

The lifetime of B_s in the 'magnetic spot' is shortened due to its small scale and low electric conductivity. The electric conductivity drops strongly towards the outermost shell of the crust because of the high density gradient (see Fig.1 in Pons & Geppert 2007).

Conventionally, the characteristic Ohmic decay time is given by

$$\tau_{\mathrm{Ohm}} = \frac{4\pi\sigma L^2}{c^2} \qquad (5)$$

where σ denotes the scalar electric conductivity and L is a typical scale length of the field structure under consideration. It is obvious, that an estimate of the magnetic field lifetime based on Eq. (5) is not well suited to describe the evolution of a such complex structure as present in the 'magnetic spot'.

More thorough analysis of poloidal field structure decay demands taking into account different field modes that form the surface field configuration. If this is done by decomposition of that structure into spherical harmonics, the following decay times are found that are marked by the multipolarity n (see Geppert et al. 2000):

$$\tau_n = \frac{4\sigma R^2}{\pi c^2 n^2} . \qquad (6)$$

Here, R denotes the radius of the sphere within which the field maintaining electric currents are circulating and σ is assumed to be homogenous throughout this sphere.

Obviously Eq. (6) is, given the constant conductivity assumption, still a rough approximation to the situation in the 'magnetic spot' too. However, it takes the complex and small scale structure of the field there better into account than Eq. (5). Clearly, the characteristic ohmic decay time τ_{0hm} overestimates the duration of field decay even for a dipolar field by about one order of magnitude. The typical scale length, i.e. the radius of dipolar field line curvature, for radio pulsars is about 10^8cm (Ruderman & Sutherland 1975). As argued above, the typical scale length of B_s has to be $\lesssim 10^6$cm.

The scale length of field structures expressed by spherical harmonics, that are determined by their multipolarity n, is for small scales related to the radius of the sphere by $L = 2\pi R/n$. For a neutron star radius $R \sim 10^6$cm and a scale of $L \equiv R_{\mathrm{cur}} \lesssim 10^6$cm, where R_{cur} denotes the field line curvature radius of B_s, returns $n \sim 10$, perhaps even significantly larger.

The electric conductivity in the layer below the surface of the 'magnetic spot' is much smaller than in somewhat deeper crustal shells. This is caused both by the high temperature $T > T_s \gtrsim 10^6$K and by the low density $\rho \lesssim 10^6$ g cm^{-3}. Extrapolating the results of Chugunov (2012) to that density range, the electric conductivity will certainly not exceed $\sigma \sim 10^{22}$s^{-1}. Thus, for a field line curvature radius $R_{\mathrm{cur}} \lesssim 1$km corresponding to a multipolarity $n \approx 10$ this electric conductivity will cause according to Eq. (6) an decay time of about 5000 years. Hence, given the lifetime of radio pulsars, the small scale field structure in the 'magnetic spot' has to be rebuilt continuously.

4.1   Structures Created at a Neutron Star's Birth

The short decay times for a poloidal field structure of $\lesssim 1$km scale length as estimated by use of Eq. (6) rule out, that such magnetic spots, occasionally created during the birth of a neutron star by small scale dynamo action, can survive over the radio pulsar lifetime. This is true the more, because during the early, say ~ 1000yrs of a neutron star's life the crustal temperature is much higher which reduces the electric conductivity additionally. Surface field anomalies created during the birth process of neutron stars can be responsible for the radio pulsar activity of very young pulsars as e.g.

the Crab-PSR. For pulsars older than $\sim 10^4$ years however, these anomalies have to be re-created continuously.

4.2 Polar Cap Currents

A potential source of magnetic spots is the possible current through the polar cap. The Goldreich-Julian charge density $n_{\rm GJ} \approx \Omega B_d/2\pi ec$. For a rotational period $P = 2\pi/\Omega = 1$ s and for $B_d = 10^{13}$ G is $n_{\rm GJ} \approx 7 \times 10^{11}$ cm^{-3}. Thus, the maximum magnetospheric current density is $j_{\rm GJ} ec \approx 10^{13}$ abamp cm^{-2}. Let's approximate Ampere's law by $B \approx (4\pi/c)j \times L$. Then, for a scale length $l \sim 10$ m the magnetic field strength $\approx 4 \times 10^7$ G. Since the required field strength at the magnetic spot should be $> 10^{13}$ G, even a much faster rotation and/or a larger scale of the field would not be sufficient to generate by magnetospheric currents a field that can cause a significant curvature of B_d at the surface of the magnetic spot.

4.3 Thermoelectric Magnetic Field Creation

Somewhat less well understood is the role that the extreme heating of the small but heavily bombarded 'hot spot' for the field evolution in the 'magnetic spot' can play. It is tiny in comparison to the whole surface and the heated layer is very shallow. The surface temperature there exceeds certainly 10^6 K while the large rest of the neutron star surface has typically a temperature of $\sim 5 \times 10^5$ K (see Page et al. 2006, for the standard cooling history). However, due to the huge meridional temperature gradient a creation and perpetuation of small scale field structures is conceivable. The battery term of the induction equation including thermoelectric effects, $\nabla Q \times \nabla T$, where Q is the predominantly radius dependent thermopower (see for details Blandford et al. 1983; Urpin et al. 1986; Geppert & Wiebicke 1991), causes the creation of a toroidal field structure. It surrounds the 'hot spot' as a torus, its inner radius corresponds roughly to the scale of the meridional temperature gradient. First estimates show, that in this torus field strength of $\sim 10^{13}$ G can be created on timescales of 10^3 years (Viganò & Pons, private communication 2013). However, this field creation process and its further interaction with crustal field structures deserves much more detailed and systematic studies.

4.4 Hall Drift in the Crust

The Hall drift in core and crust of neutron stars is subject of scientific debate since more then two decades. For the very first time the term 'Hall drift' appeared in neutron star studies by Blandford et al. (1983). They considered it as driving force that can move a field around which has been created by a thermoelectric instability in the envelope. The first who studied the effect of the Hall drift on the field decay in the crust was Jones (1988). He argued that a non-zero radial component of the Hall drift pushes magnetic flux, expelled from the superconducting core, below the neutron-drip density where it will be rapidly dissipated by Ohmic diffusion.

Later Haensel et al. (1990), Yakovlev & Shalybkov (1991), and Urpin & Shalybkov (1991) studied the influence of the Hall drift on to the Ohmic decay in the core of neutron stars. For this purpose these authors calculated the Hall components of the conductivity tensor in relaxation time approximation. These components have the same form both in the core and in the crust, the difference is made by the different relaxation times for the diverse collision processes.

Tensorial transport coefficients and the related Hall induction equation (see Eq. 7) can only be used to describe correctly the field evolution in the crystallized crust. There, the ions are fixed to the lattice sites and the electrons are the only moving charged particles - a description in terms of electron-magnetohydrodynamics is the correct one.

The more general case, when both electrons and ions (protons) can move with respect to each other and to the neutral background of neutrons has been studied in detail by Goldreich & Reisenegger (1992). In this pioneering paper they applied an (though incomplete) analogy of the Hall induction equation with the vorticity equation of an incompressible liquid to discuss the possibility, that the Hall drift causes the magnetic field to evolve in the crust through a turbulent cascade. It should create out of large scale field modes increasingly smaller ones until their scale length becomes so small, that Ohmic decay dominates the further evolution.

The realization that the thermal and magnetic evolution of neutron stars is closely related to each other is about 20 years old (see e.g. Urpin & Muslimov 1992; Urpin & van Riper 1993; Urpin et al. 1994). For the first time the magneto-thermal creation of small scale toroidal field structures close to the North pole out of a large scale one via the Hall drift in the superfluid core of neutron stars has been shown by Urpin & Shalybkov (1995).

Vainshtein et al. (2000) studied for the first time the Hall drift in a medium, where a density - and, hence, conductivity - gradient is present. Under such conditions the evolution of the toroidal field component follows a Burger's like equation which describes the creation of current sheets in low density regions, i.e. sites of very efficient field dissipation. However, even if the initial field configuration gives rise to a drift towards layers of higher conductivity, the small scale of the locally intense field causes a much faster than Ohmic dissipation of magnetic energy.

The occurrence of a Hall instability, i.e. the non-cascadic but jump-like, across wide spectral distances, transfer of magnetic energy out of large scale into small scale modes has been studied by Rheinhardt & Geppert (2002) and Geppert & Rheinhardt (2002). For the first time the creation of small scale 'magnetic spots' at the surface of neutron stars via the Hall instability has been demonstrated considering realistic crustal density profiles and cooling histories by Geppert et al. (2003) and Rheinhardt et al. (2004), however still in plan-parallel geometry. The occurrence of this instability has been disputed by Hollerbach & Rüdiger (2002) and Hollerbach & Rüdiger (2004), who extended the analytical studies of Vainshtein et al. (2000) to numerical ones, including the simultaneous presence of toroidal and poloidal crustal field components. Cumming et al. (2004) published a detailed and comprehensive study of the crustal Hall drift. They found that a purely poloidal field is not affected by that drift if its maintaining toroidal current consists of rigidly rotating electrons only; they confirmed the existence of the Hall instability and discussed whether Hall waves can strain the crust beyond its yield point. In the same year Jones (2004a) (see also Jones 2004b) explored the consequences of the existence of an amorphous phase (in contrast to an almost homogeneous body-centered cubic crystal lattice) in deep crustal layers for the creation of small scale field structures by the Hall drift. Reisenegger et al. (2007) studied both analytically and numerically the evolution of axisymmetric crustal field configurations. They showed that an exactly toroidal field is unstable to poloidal perturbations. At the expense of the much stronger toroidal field, the Hall instability leads to the creation of strong and small scale poloidal field structures close to the North pole (see Fig. 2 in Reisenegger et al. 2007). Note, that this resembles much to what we assume for

the 'initial' field configuration and to what is required to switch on a radio pulsar. A detailed study of the crustal Hall drift for various 'initial' axial symmetric field configurations, realistic microphysics, and taking into account the cooling of the crust, has been presented by Pons & Geppert (2007).

All numerical model calculations (Muslimov 1994; Naito & Kojima 1994; Shalybkov & Urpin 1997)) have been performed up to this time (see also Kojima & Kisaka 2012)) by using either a fully spectral code or a hybrid one, spectral in the angles and finite in the radial coordinate. The obtained results demonstrate the non-linear coupling between different field modes, the exchange of magnetic energy between them, and the acceleration of Ohmic diffusion. The latter occurs because the Hall drift, itself an energy conserving process, creates tendencially an increasing number of field modes with small curvatures that are subject to enhanced decay. These spectral methods, however, have very serious limitations on their applicability. Large gradients of density and temperature, as well as in the electric conductivity and magnetization parameter cause problems with the spectral resolution, especially at sites where current sheets in the crust are created.

To overcome this restrictions, in recent studies of the Hall drift another non-spectral but finite difference numerical method was used. Pons & Geppert (2010) managed to show that the Hall instability indeed can appear in plan-parallel geometry. It became clear that the field evolution during the Hall drift dominated phase proceeds not along a Hall cascade, but rather through the rapid creation of very localized small scale structures in regions where the toroidal field changes sign. In that way, possibly a Hall equilibrium will be established. For spherical and 3D symmetry however, such Hall instabilities are expected to appear in a more complicated way because a larger variety of modes can become unstable (see Reisenegger et al. 2007).

A breakthrough in the treatment of Hall drift induced shock structures has been achieved by the development and successful test of a new numerical code by the Alicante-group. A detailed and comprehensive study of this numerical method is given by Viganò et al. (2012). This code is not based on spectral methods but relies on upwind finite difference techniques that are able to handle situations with very low, even vanishing, magnetic diffusivity and overcomes the problems that are connected to the formation of sharp current sheets during the field evolution.

In the crystallized crust of neutron stars, where convective motions of the conductive material play no role, the evolution of the magnetic field is governed by the Hall–induction equation

$$\frac{\partial \vec{B}}{\partial t} = -\frac{c^2}{4\pi} \nabla \times \left(\frac{1}{\sigma} \left\{ \nabla \times \vec{B} + \omega_B \tau [(\nabla \times \vec{B}) \times \vec{b}] \right\} \right), \quad (7)$$

where $\vec{b}$ is the unit vector in the direction of the magnetic field $\vec{b} = \vec{B}/|\vec{B}|$, τ is the relaxation time of the electrons and $\omega_B = eB/m_e c$ is the electron cyclotron frequency. Here, σ is the electrical conductivity parallel to the magnetic field (independent of the magnetic field strength).

The Hall drift term at the r.h.s. of Eq. (7) is a consequence of the tensorial properties of the electric conductivity in the presence of a magnetic field. The tensor components of the electric conductivity are derived in the relaxation time approximation (Yakovlev & Shalybkov 1991).

If the *magnetization parameter* ($\omega_B \tau$) exceeds unity significantly, the Hall drift dominates the ohmic diffusion and will result in a very different field evolution. A large magnetization parameter, typically ≈ 1000 during some stages (see Figs. 1 in Geppert

& Rheinhardt 2002, and also Pons & Geppert 2007), strongly suppresses the electric conductivity perpendicular to the magnetic field and changes the character of Eq. (7). The magnetization parameter

$$\omega_B \tau = \frac{eB(r,\theta,t)}{m_e^*(r)c} \tau[\rho(r), T(r,\theta,t), Q(r), A(r), Z(r)] \quad (8)$$

depends on quantities that are in the present approximation functions of the radial coordinate only, as the density ρ, the charge number Z, the mass number A, the impurity concentration Q, and the effective electron mass m_e^*. Due to the certainly non-monopolar crustal magnetic field the heat flux through the crust will not be spherically symmetric (Geppert et al. 2004; Pérez-Azorín et al. 2006). Hence, the temperature T depends on the radial and on the meridional coordinate. Additionally, the magnetization parameter is linear in the magnetic field itself. This makes $\omega_B \tau$ to a spatially and temporally strongly varying quantity.

4.5 Initial magnetic field configuration

A basic feature of the Hall drift is the interaction between field modes that are different in their geometry - toroidal or poloidal - and in their scale. The way how the Hall drift affects the field evolution depends strongly on the initial field configuration. The meaning of 'initial' is not unambiguously. It is reasonable either to chose a moment very close to the neutron star birth or the moment, when $\omega_B \tau$ exceeds unity. The importance of the initial field geometry is demonstrated by the fact that, if there is initially only a purely toroidal field component present, in axial symmetry never poloidal field modes will be created. In the opposite case, the sole existence of poloidal modes in the initial field, the Hall drift will create out of them toroidal field components.

The precondition for the creation of the required 'magnetic spot' is the initial existence of a standard large scale, i.e. dipolar poloidal field B_d, whose last open field lines determine the area of the canonical polar cap. For the Hall drift to act efficiently, additionally a strong toroidal field B_{tor} must be present too. The idea that in the crust resides a very strong toroidal field is gaining more and more support (see e.g. Halpern & Gotthelf 2010; Shabaltas & Lai 2012; Viganò & Pons 2012). The open question is its structure. It has to fill almost the whole crust. Moreover, it has to reside in deeper layers of the crust where the conductivity is high enough to guarantee a lifetime exceeding well 10^6 years but not too deep, where a hypothetical 'pasta'-phase with a huge impurity parameter can accelerate the toroidal field decay (see Jones 1999, 2001; Pons et al. 2013). That is to say that B_{tor} has to be concentrated not only to a small equatorial belt, as MHD equilibrium models suggest, but is strong as well in higher latitudes, closer to the poles. Our preferred initial field configuration can have the form shown in the left panel of Fig.2. At the axial symmetric level of field evolution modeling, initial toroidal field structures that are concentrated only in the equatorial plane do not provide the required strong small scale field structures on acceptable time scales.

It is still unclear whether an initial field configuration with an extended toroidal component actually exists in the crusts of neutron stars which continue their life as radio pulsars. Studies of the MHD equilibrium in still liquid, newborn neutron stars argue against it (Braithwaite & Spruit 2004; Lyutikov 2010; Glampedakis et al. 2012; Lander & Jones 2012; Fujisawa et al. 2012). An interesting attempt to conclude about the internal field configuration by analyzing the magneto-elastic oscillation of neutron stars has been made recently by Gabler et al. (2013). In two very recent publications
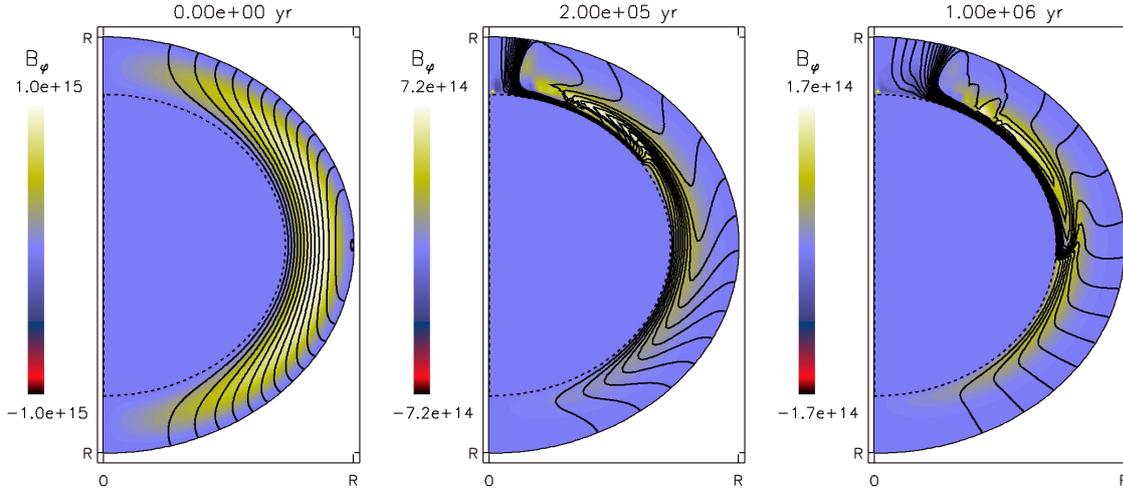
Figure 2. Structure of the crustal magnetic field at $t = 0$ (left), after 2×10^5 (middle) and after 10^6 yrs (right). The poloidal field is shown by solid lines, the isolines of the toroidal field are color coded. The crustal region has been stretched by a factor of 4 for visualization purposes. The complete movie showing the field dynamics is available at *http://personal.ua.es/en/daniele-vigano/hall-pulsar.html*. At the same address a movie cab be seen that shows the evolution of the external field lines; with and without the effect of the Hall drift too.

Gourgouliatos et al. (2013a,b) studied in axial symmetry the transition from MHD equilibrium, established in barotropic matter, to a Hall equilibrium. Both equilibria are characterized by a toroidal field that is confined to an equatorial belt, not extending to very high latitudes. There are, however, also observational hints, that the crustal toroidal field has a structure similar to that assumed by us (Rea et al. 2010; Shabaltas & Lai 2012)). Small scale dynamos, as suggested by Thompson & Duncan (1993), could be a viable mechanism that creates a toroidal field everywhere in the crust. Conceivable is also, that the submergence of a MHD equilibrium field during the supernova fallback creates the required toroidal field (Geppert et al. 1999; Ho 2011; Viganò & Pons 2012; Bernal et al. 2013). The question about the initial field configuration will be certainly subject of the future scientific debate. However, the very existence of radio pulsars should be taken into account then.

5 MAGNETIC FIELD EVOLUTION IN THE CRUST

As in the neutron star core, the magnetic field evolution in the crust cannot be considered detached from the thermal history (see e.g. Aguilera et al. 2008; Pons et al. 2009; Viganò et al. 2013, and references therein). Both quantities, temperature and magnetic field, are intimately connected with each other there. The electric conductivity in the crystallized crust decreases strongly with increasing temperature temperature (see Fig. 1 in Pons & Geppert 2007). Thus, the hotter the crust, the faster the magnetic field decay. The magnetic field itself affects the cooling of the crust, either by channeling the heat flow along the field lines and/or by being a Joule heat source. Since the Hall drift causes the creation of small scale field structures, these are sites of enhanced Joule heating and sites of accelerated field decay too.

Physically, the Hall drift couples the field creating currents with the field itself in a non-linear manner. This coupling creates in an energy conserving manner small scale field structures out of large scale ones. Without the Hall drift, the initial magnetic field configuration would be stable, being subject only to Ohmic diffusion. Mathematically, the Hall induction equation changes its character both spatially and temporally during the whole process of crustal field evolution quite rapidly. In regions and in periods where Ohmic dissipation dominates, Eq. (7) is a parabolic differential equation. However, where and when the magnetization parameter $\omega_B \tau \gg 1$, Eq. (7) becomes a hyperbolic one. This behavior causes not only severe numerical problems. It makes also any analytic approach to describe the total crustal field evolution e.g. in terms of ideal MHD questionable. A realistic idea about the effects of the Hall drift on to the field evolution within the the crust, where steep density gradients and a huge thermal inhomogeneity are present, can only be achieved by sophisticated numerical modeling.

The presently most advanced way to model the magneto-thermal evolution of the crust is to use the above mentioned code of the Alicante-group (Viganò et al. 2012). A successful application of this code has been published recently by Viganò et al. (2013). These authors were able to explain the observational diversity of isolated neutron stars in the framework of the magneto-thermal evolution which is described just by that code.

In order to solve Eq. (7), the Alicante-group code has been applied. Since this code is especially able to handle the specifics of the Hall drift it is well-suited to study the crustal field evolution during the first 10^6 years of a neutron star's life. The 'initial' magnetic field structure consists of a poloidal dipolar field with a polar surface strength of 10^{13} G. It has very little effect on to the development of 'magnetic spots' whether this large scale poloidal field is anchored in the crust or is a core centered one. Important is the existence of a strong toroidal field component that has to reside in deeper layers of the crust in order to survive a period of $\sim 10^6$ years almost undecayed. The 'initial' toroidal field shown in the left panel of Fig.2 has a maximum strength of 10^{15} G.

In the middle and right panels of Fig.2 snapshots of the crustal field structure after 2×10^5 and 10^6 years are shown. Obviously, strong and small scale surface field components are created close to the North pole and can be maintained over $\sim 10^6$ years. The axial symmetry is still conserved although there appears an extreme asymmetry between the field structures near the North- and South-

pole. This asymmetry is caused by the symmetry of the initial magnetic field configuration adopted in our calculations (left panel). While the Hall drift velocity is proportional to the field strength, the initial field symmetry determines a preferred Hall drift direction. It points towards one of the poles depending on the relative sign of the toroidal field with respect to the poloidal one. In our case we have chosen the negative signature that resulted in the drift towards the North pole. Of course, the opposite direction is equally likely. However, we will argue later on, that the initial dipolar configuration is the only one that produces the required magnetic spots on a proper timescale.

The role which the initial field configuration plays is best discussed by considering two qualitatively different magnetic field configurations: dipolar and quadrupolar. As Pons & Geppert (2007) emphasized, there are two main effects that determine the crustal field evolution, especially if there is initially a strong toroidal field component present. It is globally displaced toward the inner crust following the negative conductivity gradient. Depending on the relative sign with respect to the poloidal component it tends to move meridionally to one or the other magnetic pole. In case of the initial toroidal field would have a geometry which is about quadrupolar, that motion would be North-South symmetric and directed towards the equatorial plane.

For example, the evolution of a crustal field that consists of initially almost dipolar toroidal and poloidal components is demonstrated in the second row of Fig. 6 in Viganò et al. (2013). The 'magnetic spot' has typically a meridional extent of a few degrees which corresponds to a few hundred meters on the surface. A qualitatively different situation is presented in Figs. 2 and 3 of Pons & Geppert (2007), where the initial toroidal field adopted in calculations has a quadrupolar structure but the poloidal component remains dipolar. In this case the Hall drift is equatorial symmetric and directed from either pole towards the equatorial plane, creating there small scale structures. [1]

Since the crustal conductivity profile is qualitatively similar for all isolated neutron stars, the location of the 'magnetic spot' depends crucially on the initial magnetic field geometry. Spots can be created at various latitudes, provided the initial magnetic field has the corresponding structure. The term in the induction equation that describes the meridional drift motion and the compression of field lines is of course the Hall drift term. The Ohmic diffusion term describes the global trend of the toroidal field to migrate toward deeper crustal regions with higher electric conductivity.

As it has been shown in Section 3, the quantities that are responsible for a sufficient creation of electron-positron pairs are the surface field strength in the 'magnetic spot', B_s, and the radius of curvature of the field lines there, R_{cur}, which are connected to the open dipolar lines along which the charges can be accelerated to relativistic velocities within the polar gap. These quantities (B_s and $R_{cur} = \left(-(\vec{b} \cdot \nabla)\vec{b} \right)^{-1}$) are presented in Fig. 3. To show the striking effect of the Hall drift, the field evolution as would appear without it (being subject only to Ohmic diffusion) is indicated by dashed lines. Without Hall drift B_s would decrease slowly from about 10^{13} G and the R_{cur} would remain almost stable at a value of a few hundred kilometers, a value typical for dipolar fields. The realistic situation is presented by solid lines. For the initial field

---

[1] One should notice that the upper limit for the size of the 'magnetic spot' is the crust thickness which is about 1 km, consistent with our numerical results mentioned just above. It is worth emphasizing here, that 'magnetic spot' and 'hot spot' are different entities.

strengths considered here (maximum toroidal field 10^{15} G, polar surface poloidal field 10^{13} G) a 'magnetic spot' is created on a Hall time scale $\tau_{Hall} \sim 10^{3-4}$ years.

The Hall drift is a quite agile process that causes relatively rapid variations on the Hall time scale in that spot; between a time step of 10000 years the maximum of B_s and the minimum of R_{cur} varies by about $1°$ within the spot. Since it is unimportant where within the 'magnetic spot' the strongest B_s and the smallest R_{cur} are located at a given moment, both B_s and the minimum of R_{cur} are averaged over a meridional range of about $5°$, which is presented in Fig.3.

The results presented in Figs. 2 and 3 prove, that the for the functioning of radio pulsar emission necessary field structures are created on a reasonable time scale: field strengths well exceeding 10^{13} G and curvature radii much smaller than a few 100 km. Moreover, an increase of the maximum strength of the initial toroidal field increases the strength of the spot field too. Therefore, the resultant spot field can exceed 10^{14} G for a longer period of time. However, there is an upper limit for the crustal toroidal field strength. Indeed, an increase of the field is associated with an increase of the Joule heating and when the strength reaches about 5×10^{15} G the Joule heating leads to an enhanced Ohmic dissipation of the total crustal field.

The Hall drift tends always to create out of an initially large scale field a field of much finer structure. We have, however, to emphasize, that the here presented initial crustal magnetic field geometry is the only one in the manifold of examined ones that provides the required 'magnetic spot' within $\sim 10^4$ years surviving a typical pulsar lifetime $\gtrsim 10^6$ years. It is likely that the number of favorable initial field structures increases when 3D models can be calculated in the future.

6   CONCLUSIONS

Our ideas and results can be comprised in the following chain of reasoning:

(i) The brightness temperature of pulsar radio emission implies that a coherent radiation mechanism must be involved, which requires creation of very dense, relativistic electron-positron plasma above the polar cap.

(ii) The inner pulsar acceleration region exists just above the polar cap, presumably in the form of PSG.

(iii) To create a large enough number of electron-positron pairs the curvature radius of surface magnetic field lines within PSG has to be $\lesssim 10^6$ cm, i.e. the magnetic field structure has to be a 'magnetic spot' kind.

(iv) PSG can be created only if the cohesive energy of charges at the polar cap surface exceeds some critical value which is determined by the strength of the local magnetic field.

(v) Combined radio and X-ray observations of several pulsars indicate that the actual polar cap, above which the acceleration arises, has a much smaller size than the canonical polar cap.

(vi) The surface temperature of the spot T_s is of the order of 10^6 K, which exceeds by far a typical surface temperature corresponding to a cooling age of $\sim 10^6$ years. Thus, this temperature results from back flow bombardment of the actual polar cap.

(vii) Both the small size of the actual polar cap (flux conservation arguments) and its high T_s indicate that the strength of the surface magnetic field B_s is a of the order of 10^{14} G.
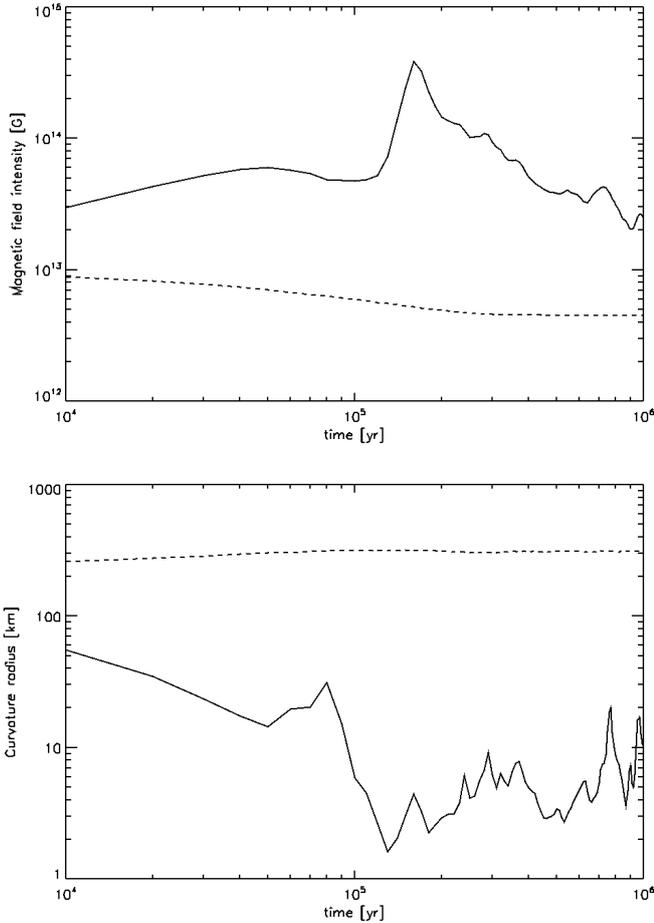
Figure 3. Temporal evolution of B_s (upper panel) and $R_{\rm cur}$ (lower panel) near the north pole, considering only Ohmic dissipation (dashed) or including the Hall term (solid). We show averages of the numerical values of B_s and the minimum of $R_{\rm cur}$ in the region $1° - 5°$ from the north pole.

(viii) Such a magnetic field anomalies have to be maintained over a pulsar lifetime of $\sim 10^6 - 10^7$ years, at least in the polar cap region. Thus, small scale field structures created at a neutron star's birth are ruled out. The polar cap currents also can not be responsible for such a field.

(ix) To our knowledge, the only mechanism that can provide the strong, small scale magnetic field structures is the Hall drift. It couples non-linearly a standard large scale poloidal field ($10^{12} - 10^{13}$ G) and a toroidal field that resides in deeper layers, occupying almost the whole crust with a maximum strength of $\sim 10^{15}$ G.

(x) Model calculations, although performed only in axisymmetric geometry, show, that the field structures necessary for the pulsar radio emission can be created on the right time scale and with the required field strength via the Hall drift.

We should now point out possible caveats of our idea. The first problem concerns location of the line that separates "Gap" - "No Gap" regions in Fig. 1. This line describes dependence of the critical temperature (Medin & Lai 2007) on the magnetic field strength. Since Medin & Lai (2007) calculated the binding energy for iron ions within an accuracy of a few tens of a per cent, this curve might be slightly shifted towards the lower values for a given magnetic

field strength. However, all calculations are certainly correct in the sense of an order of magnitude estimates.

Also Zhang et al. (2005), Kargaltsev et al. (2006) and Pavlov et al. (2009) pointed out, the black-body fits that return both $A_{\rm BB}$ and T_s are based on a small photon number statistics and have about the same quality as power law fits indicating a magnetospheric origin of the radiation. Nevertheless, we believe that both the gap formation conditions and the corresponding observational hints that these conditions are fulfilled are quite convincing to justify our assumptions. On the other hand, one should realize that the pair creation process is also associated with the synchrotron magnetospheric radiation, so the power law component must be present in the composite spectrum.

Another problem is the restriction of the model calculations to axial symmetry. We expect that a future more realistic 3-dimensional treatment of the Hall effect in a neutron star's crust will provide an even better coincidence with observations. Then, the 'magnetic spot' will occur as a real spot, restricted both in meridional and azimuthal direction. This will make possible to describe the real shape and size of the actual polar gap.

REFERENCES

Aguilera D. N., Pons J. A., Miralles J. A., 2008, ApJL, 673, L167
Arons J., Scharlemann E. T., 1979, ApJ, 231, 854
Asseo E., & Melikidze G. I. 1998, MNRAS, 301, 59
Bernal C. G., Page D., Lee W. H., 2013, ApJ, 770, 106
Blandford R. D., Applegate J. H., Hernquist L., 1983, MNRAS, 204, 1025
Braithwaite J., Spruit H. C., 2004, Nature, 431, 819
Cheng A. F., Ruderman M. A., 1977, ApJ, 214, 598
Chugunov A. I., 2012, Astronomy Letters, 38, 25
Cumming A., Arras P., Zweibel E., 2004, ApJ, 609, 999
Fujisawa K., Yoshida S., Eriguchi Y., 2012, MNRAS, 422, 434
Gabler M., Cerdá-Durán P., Font J. A., Müller E., Stergioulas N., 2013, MNRAS, 430, 1811
Geppert U., Gil J., Melikidze G., Pons J., Viganò D., 2012, in Lewandowski W., Maron O., Kijak J., eds, Astronomical Society of the Pacific Conference Series Vol. 466 of Astronomical Society of the Pacific Conference Series, Hall Drift in the Crust of Neutron Stars - Necessary for Radio Pulsar Activity?. p. 187
Geppert U., Küker M., Page D., 2004, A&A, 426, 267
Geppert U., Page D., Zannias T., 1999, A&A, 345, 847
Geppert U., Page D., Zannias T., 2000, Physical Review D, 61, 123004
Geppert U., Rheinhardt M., 2002, A&A, 392, 1015
Geppert U., Rheinhardt M., Gil J., 2003, A&A, 412, L33
Geppert U., Wiebicke H.-J., 1991, Astron. Astrophys. Suppl., 87, 217

Gil J., Haberl F., Melikidze G., Geppert U., Zhang B., Melikidze Jr. G., 2008, ApJ, 686, 497

Gil J., Lyubarsky Y., Melikidze G. I., 2004, ApJ, 600, 872

Gil, J. A., Melikidze, G. I. & Mitra, D., 2002, A&A, 388, 235

Gil J., Melikidze G., Zhang B., 2007a, Ap&SS, 308, 325

Gil J., Melikidze G., Zhang B., 2007b, MNRAS, 376, L67

Gil J., Melikidze G. I., Geppert U., 2003, A&A, 407, 315

Glampedakis K., Andersson N., Lander S. K., 2012, MNRAS, 420, 1263

Goldreich P., Julian W. H., 1969, ApJ, 157, 869

Goldreich P., Reisenegger A., 1992, ApJ, 395, 250

Gourgouliatos K. N., Cumming A., Reisenegger A., Armaza C., Lyutikov M., Valdivia J. A., 2013, MNRAS, in press, ArXiv e-prints 1305.6269

Gourgouliatos K. N., Cumming A., Lyutikov M., Reisenegger A., 2013, ArXiv e-prints 1305.0149

Haensel P., Urpin V. A., Yakovlev D. G., 1990, A&A, 229, 133

Halpern J. P., Gotthelf E. V., 2010, ApJ, 709, 436

Hermsen W., Hessels J. W. T., Kuiper L., van Leeuwen J., Mitra D., de Plaa J., Rankin J. M., Stappers B. W., Wright G. A. E., 2013, Science, 339, 436

Ho W. C. G., 2011, MNRAS, 414, 2567

Hollerbach R., Rüdiger G., 2002, MNRAS, 337, 216

Hollerbach R., Rüdiger G., 2004, MNRAS, 347, 1273

Jackson J., 1975, Classical Electrodynamicss. New York: Willey

Jones P. B., 1988, MNRAS, 233, 875

Jones P. B., 1999, Physical Review Letters, 83, 3589

Jones P. B., 2001, MNRAS, 321, 167

Jones P. B., 2004a, Physical Review Letters, 93, 221101

Jones P. B., 2004b, MNRAS, 351, 956

Kargaltsev O., Pavlov G. G., Garmire G. P., 2006, ApJ, 636, 406

Kojima Y., Kisaka S., 2012, MNRAS, 421, 2722

Lander S. K., Jones D. I., 2012, MNRAS, 424, 482

Lyutikov M., 2010, MNRAS, 402, 345

Medin Z., Lai D., 2007, MNRAS, 382, 1833

Melikidze G. I., Gil J. A., Pataraya A. D., 2000, ApJ, 544, 1081

Mereghetti S., Tiengo A., Esposito P., Turolla R., 2013, MNRAS, in press, ArXiv e-prints 1308.0506M

Muslimov A. G., 1994, MNRAS, 267, 523

Naito T., Kojima Y., 1994, MNRAS, 266, 597

Page D., Geppert U., Weber F., 2006, Nuclear Physics A, 777, 497

Pataraia A. & Melikidze G., 1980, Ap&SS, 68, 61

Pavlov G. G., Kargaltsev O., Wong J. A., Garmire G. P., 2009, ApJ, 691, 458

Pérez-Azorín J. F., Miralles J. A., Pons J. A., 2006, A&A, 451, 1009

Pons J. A., Geppert U., 2007, A&A, 470, 303

Pons J. A., Geppert U., 2010, A&A, 513, L12+

Pons J. A., Miralles J. A., Geppert U., 2009, A&A, 496, 207

Pons J. A., Viganò D., Rea N., 2013, ArXiv e-prints 1304.6546P

Rea N., Esposito P., Turolla R., Israel G. L., Zane S., Stella L., Mereghetti S., Tiengo A., Götz D., Göğüş E., Kouveliotou C., 2010, Science, 330, 944

Reisenegger A., Benguria R., Prieto J. P., Araya P. A., Lai D., 2007, A&A, 472, 233

Rheinhardt M., Geppert U., 2002, Physical Review Letters, 88, 101103

Rheinhardt M., Konenkov D., Geppert U., 2004, A&A, 420, 631

Ruderman M. A., Sutherland P. G., 1975, ApJ, 196, 51

Shabaltas N., Lai D., 2012, ApJ, 748, 148

Shalybkov D. A., Urpin V. A., 1997, A&A, 321, 685

Szary A., 2013, ArXiv e-prints 1304.4203

Szary A., Melikidze G. I., Gil J., 2010, in Proceedings of High Time Resolution Astrophysics - The Era of Extremely Large Telescopes (HTRA-IV). May 5 - 7, 2010. Agios Nikolaos, Crete Greece. Partially Screened Gap - general approach and observational consequences

Thompson C., Duncan R. C., 1993, ApJ, 408, 194

Urpin V. A., Chanmugam G., Sang Y., 1994, ApJ, 433, 780

Urpin V. A., Levshakov S. A., Iakovlev D. G., 1986, MNRAS, 219, 703

Urpin V. A., Muslimov A. G., 1992, Soviet Astronomy, 36, 530

Urpin V. A., Shalybkov D. A., 1991, Sov. Phys. JETP, 73, 703

Urpin V. A., Shalybkov D. A., 1995, A&A, 294, 117

Urpin V. A., van Riper K. A., 1993, ApJL, 411, L87

Vainshtein S. I., Chitre S. M., Olinto A. V., 2000, Physical Review E, 61, 4422

Viganò D., Pons J. A., 2012, MNRAS, 425, 2487

Viganò D., Pons J. A., Miralles J. A., 2012, Computer Physics Communications, 183, 2042

Viganò D., Rea N., Pons J. A., Perna R., Aguilera D. N., Miralles J. A., 2013, MNRAS, in press

Yakovlev D. G., Shalybkov D. A., 1991, Ap&SS, 176, 191

Zhang B., Sanwal D., Pavlov G. G., 2005, ApJ, 624, L109